The Earliest Stages of Wind Wave Generation in the Open Sea

Luigi Cavaleri[a], Sabique Langodan[b], Paolo Pezzutto[c], and Alvise Benetazzo[a]

[a] *Institute of Marine Science, CNR-ISMAR, Venice, Italy*
[b] *King Abdullah University of Science and Technology, Thuwal, Saudi Arabia*
[c] *Institute for Marine Biological and Biotechnological Resources, CNR-IRBIM, Ancona, Italy*

ABSTRACT: We have explored the earliest stages of wind wave generation in the open sea, from the first initial wavelets appearing on an otherwise flat surface or low, smooth undulations until the practically fully developed conditions for the very low range of wind speeds we have considered. We suggest the minimal wind speed for the appearance of the first wavelets to be close to 1.8 m s^{-1}. The peculiar conditions associated with the development of coastal sea breezes allow us to consider the local waves as generated under time-limited conditions. The 2D spectra measured during these very early stages provide the first evidence of an active Phillips process generation in the field. After appearing in these very early stages, wavelets quickly disappear as soon as the developing wind waves take a leading role. We suggest that this process is due to the strong spatial gradients in the surface orbital velocity, which impedes the instability mechanism at the base of their formation, while at a later stage of development, these gradients decrease and wavelets reappear. On a decadal perspective, the progressive decrease of the intensity of the sea breezes in the northern Adriatic Sea, where we have carried out our measurements, is associated with the steadily milder winters, and therefore not sufficiently cold local sea temperatures in early summer.

SIGNIFICANCE STATEMENT: We have explored for the first time the earliest stages of wind wave generation (millimeter scale) in the open sea. This was possible with the combination of the daily sea breeze development and the availability of an oceanographic tower 15 km offshore. The minimum wind speed for wave generation was 1.8 m s^{-1}, lower than previously assumed. The data provide strong indications on the different stages of the generation process, offering measured and visual evidence, under these very light wind conditions, of the Phillips one. The presence of wind-related ripples, essential for remote sensing measurements, turns out to be dependent on the stage of generation.

1. The framework of an idea and its application

Surface gravity waves are generated by wind, though not continuously and not uniformly on an infinite ocean. For this reason, most of the time we deal with either time- or space-limited generation. Classical experiments, in a wind wave tank or in the field (the obvious references are JONSWAP, i.e., Hasselmann et al. 1973; Snyder et al. 1981; Babanin et al. 2007), have their limit in the spatial extent of the available field. Extended, ideal time-limited generation is practically nonexistent in the open ocean. Waves are practically ubiquitous, and in any case, wind does not appear out of the blue in the whole area of interest. On the other hand, we feel that time-limited generation should be the natural way to approach the problem. It is an enlightening experience to follow its earliest (20–30 s) stages in a wind wave tank.

One of us (LC) spent much time on the Institute of Marine Sciences of the National Research Council of Italy (CNR-ISMAR, henceforth ISMAR) oceanographic tower "Acqua Alta" (shown in Fig. 3). The interest was in measuring waves in a storm, but the

activity also implied an extensive presence on board in all seasons. Sea breezes are a common phenomenon along most of the sunny coastlines. Particularly in early summer, when still relatively cold seawater and a well-sunned land are present, coastal breezes develop and blow for a few hours. The classical sequence (see, e.g., Miller et al. 2003) is a progressive extension in time, both inland and offshore, of the affected area. This varies depending on the conditions, reaching in some places up to 200 km offshore (see, e.g., Aboobacker et al. 2014). Wind speed can be considerable, reaching 6–7 m s^{-1} (see Fig. 1), at least time ago, also in the enclosed upper end of the Adriatic Sea (soon to be shown). The evidence is that, following a progressive beginning at the coast, at an offshore point the wind appears locally almost as a step function. On the sea, the increasing extension of the affected area acts as a "front" moving offshore.

The area where we focus our attention is shown in Fig. 2, i.e., at the upper end of the Adriatic Sea, east of Italy (see the little rectangle on the left panel, then enlarged in the right one, to show the Venice lagoon and the position of the Acqua Alta tower 15 km off the coast). The local depth is 16 m, the bottom is practically flat, with a gentle slope (1/1000) toward the coast. We have no modeling of the breeze development, but the direct experience on the tower suggests an interesting possibility.

Time-limited generation implies that, starting at time 0, the waves reaching the measurement position at time T had been

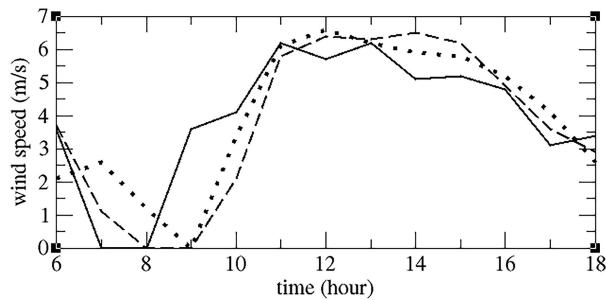*Corresponding author*: Luigi Cavaleri, luigi.cavaleri@cnr.it

FIG. 1. Examples of how strong sea breezes used to be at the ISMAR oceanographic tower (see Fig. 3). Data derived from sparse original ink on paper records, 1974. The present corresponding conditions are much milder.

generated for a T or less extended time. With waves due to breeze, the condition for this is that the front moves offshore with a speed greater than the group speed of the measured waves. This turns out to be the case, at least in our area of interest, because, as an example, the energy of 3-s waves moves at less than 2.5 m s^{-1}, i.e., 9 km h^{-1}, while the speed of the front is substantially larger (see Rafiq et al. 2020). More so because the assumed 3-s waves began as wavelets, and their average group speed along their generation time is lower than when measured at the tower.

As seen in Fig. 1, sea breezes used to be rather energetic. However, in the year (2008) we carried out the experiments, the conditions were suitable, but not so energetic. Indeed, our breezes were on the order of 2–3 m s^{-1}. As we will see, this was sufficient for wave generation, in so doing also touching on the subject of the required minimal wind speed and the wave spectra in these very early stages.

In the following, we provide a description of the experiment, of the measurements we managed to achieve, and of the corresponding main results. More in detail, section 2 describes the instrumental setup, its limits, and capability. The basic theory for wind wave generation is briefly reviewed in section 3, with a particular focus on its earliest stages. Section 4 describes the three days of data, the situation, the practical problems, what we achieved, and what we have. In section 5 we present our basic results, with a keen description of the situation, far from the more energetic ones we had hoped for, but suitable to lead to interesting results. These are discussed in section 6, where the long-term experience on board also leads to some climatic considerations. The basic results are itemized in the final section 7.

2. The area and the instrumental setup

a. The local area and the situation

The area is shown in Fig. 2. The tower, the small dot in the right panel, is shown in Fig. 3. The two panels provide the same perspective of the structure, respectively: left, when the measurements were carried out; right, after the 2018 renovation. Stormy waves can be pretty high, with 6-m significant wave height and 12-m maximum single height, both bottom limited, higher when the storm is superimposed to the locally common storm surges (see, e.g., Cavaleri et al. 2019, 2020).

The tower, set into position in March 1970, had a 7-m-long horizontal extension (visible in both the panels) at the second floor (third after the renovation), 7 m above the mean sea level (in the left panel), where also the power generators are located. This floor had been heavily damaged during a severe storm in 1979 (see Cavaleri et al. 2010), so the working part of the tower
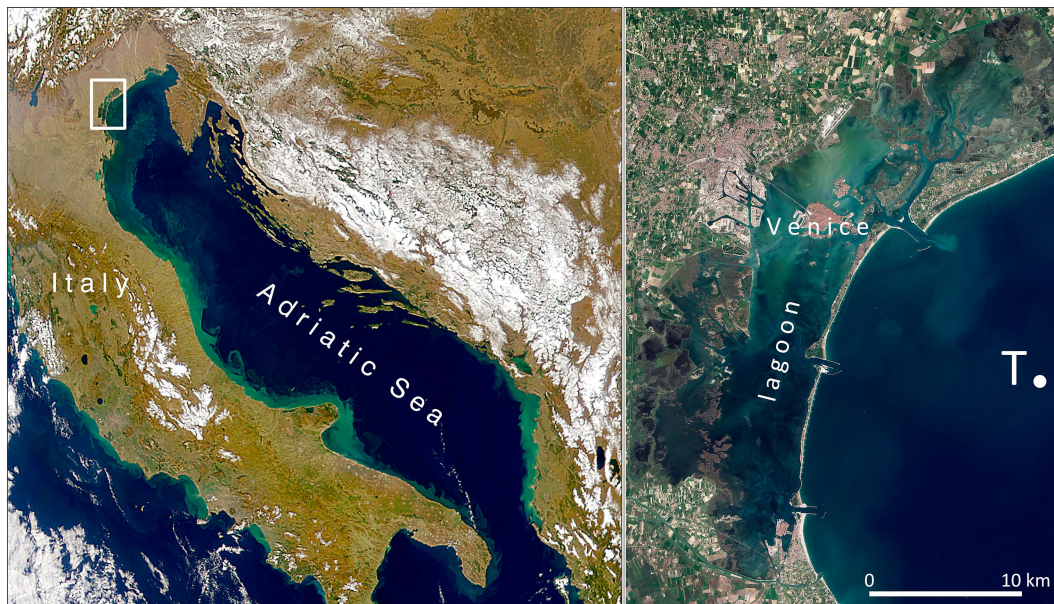

FIG. 2. (left) Italian peninsula with the Adriatic Sea on its east side. (right) Zoom-in of the area in front of the Venice lagoon (shown by the little rectangle in the left panel). The dot points to the position of the ISMAR oceanographic tower.

FIG. 3. The ISMAR oceanographic tower Acqua Alta. (left) The original structure used during the measurements; (right) after the restoration in 2018. The emerged working part is now 2 m higher. See Fig. 2 for its position.

has been raised by 2 m in the renovation of 2018, while keeping the basic holding structure. The horizontal extension, as in the right panel, is therefore 9 m above the mean sea level at present.

In summer, the meteorological situation is generally dominated by a high pressure zone, without significant winds, except for occasional thunderstorms. The sea is typically calm, without relevant waves. Occasional low waves cross the area, due to what a former fisherman, then in charge, when on board, of the tower daily operations, used to define "venti persi" (lost winds). In clear calm weather there is a night breeze, typically from the northeast. After this disappears in the early morning, there is a short calm before the southeast sea breeze begins. This lasts until late in the afternoon, slowing down when the sun's heating progressively decreases. This is the classical cycle, with many small variations.

The measuring instruments were located on the vertical of the outer end of the second floor 7-m-long extension. Facing the incoming breeze direction, this was the best position to minimize the effects of the structure on the measurements. Cavaleri and Zecchetto (1987) reported measuring the reflection from the tower frame and finding it practically absent, the more so for the minor waves we are here interested in. Apart from any other consideration, the main reason is the thick layer of mussels on the tower legs ensuring the lack of any practical reflection toward the measuring instruments.

b. The instrumental setup

Two thick wires were vertically tensed from the outer end of the then 7-m-high platform (Fig. 3, left) to the bottom. These were used as guides for a sliding cart (Fig. 4, photo and geometry). A swinging frame, visible in Fig. 3 on its horizontal position, was turned vertical when required, allowing a direct

handling of the cart. Eight thin (diameter $\Phi = 1$ mm) capacitance wave gauges, about 1 m long, were vertically tensed. Their geometrical distribution is in Fig. 4. The aim was to have two sets of very close gauges at the corners of a 2-cm square, and a triplet (e.g., 1, 5, 8) at a larger distance. The obvious purpose was to measure the directional characteristics of both the short and long waves.

To avoid any interference, only batteries were used, with no power generator at work. The hardware and the gauge material were provided by Mark Donelan. The capacitance wire was specially manufactured. The thickness of the insulating material was constant within very narrow limits. The verified ensuing calibration was linear at better than 1%.

We came across several problems (as usual and expected). The connection gauge cable proved critical, so only gauges 2, 3, 4, 5, 6, 8 were working properly. From the mechanical point of view, the asymmetry of the cart with respect to the two guiding vertical wires implied a nontrivial yaw motion also with 0.1–0.2-m-high waves. This was fixed by adding a movable rigid connector with the swinging frame.

The signals were recorded at an uneven sampling rate, close to 32 Hz, hence not directly suitable for discrete Fourier transform. The time series were then resampled over an evenly spaced time grid via a Voronoi–Allebach approach (Sauer and Allebach 1987), checking the consistency with the original signal features up to 20 Hz, doubling the maximum frequency of practical interest (10 Hz). The calibration of the single gauges was done first in the laboratory, then, granted a calm day, also at the tower via repetitive short records with intermediate assigned vertical shifts of the cart.

During measurements, typically sequences of six records were taken, each one of either 5- or 10-min duration. Wind
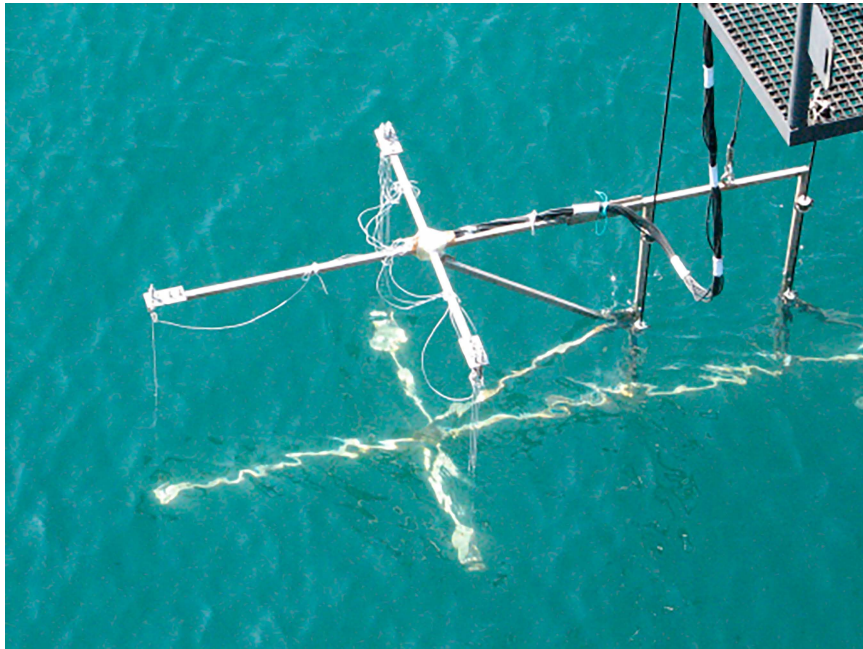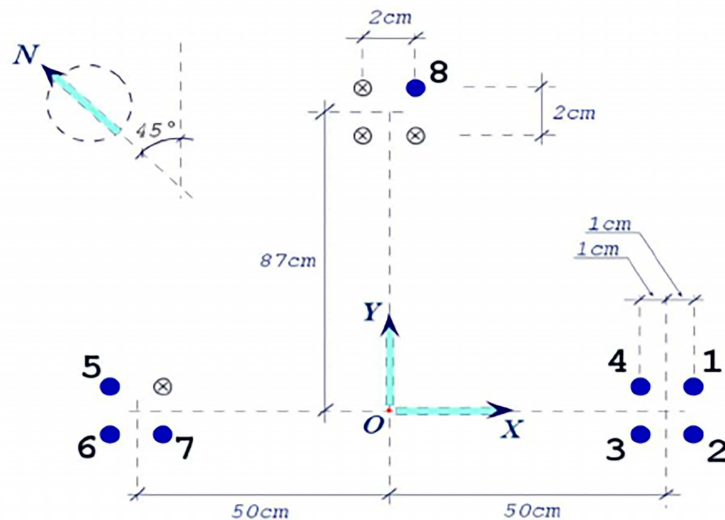
FIG. 4. The cart used for and during the measurements, and the geometry of the wave gauges distribution.

was continuously recorded at 15-m height, 3 m above the top of the tower. The kinematic influence of the structure was taken into account (Cavaleri et al. 1985). In a somewhat less conventional albeit more informative way, we dropped little pieces of paper from a position at 8-m height at the outer end of the horizontal platform. The time required to reach the surface provided the falling speed. At the same time, we carefully measured the trajectory angle with respect to the vertical and the surface touch point (videos available). This provided a nonorthodox, but very accurate estimate, also suggesting a constant wind speed from 8-m height to the surface. This is consistent with Carpenter et al. (2022), who showed that, in similar conditions, the critical layer of the Miles (1957) generation process is almost adherent to (1 mm away from) the wavy surface. We refer to these data as WTP ones.

Current measurements were taken continuously during the records. Data were available from an ADCP located 20 m east of the tower. However, these data were available only a posteriori and not representative of the surface layer, the one affecting the short waves we cared about. For the latter

purpose, we again resorted to dropping little pieces of paper on the surface and then measuring their drift. Fully immersed (hence not driven by wind) and monitored for 1 min, they provided a sufficiently precise (5% error) estimate of the surface current. We refer to these as CTP data. All the spectra we show are with respect to the current (in any case often trivial or absent). In practice, current was fully taken into account into our analysis and results, both for waves and relative wind. In general, currents, at a level potentially affecting our measurements, were practically absent most of the time, with only occasional short bursts, up to 0.20 m s^{-1} at most. Data taken during these bursts are not considered in the following sections.

3. Wind wave generation

After the nineteenth century interactions between H. von Helmholtz and W. Thomson (later Lord Kelvin), in the twentieth century the subject of wave generation by wind was taken up by Jeffreys (1925). However, his sheltering hypothesis could not quantitatively justify the evidence available from the field. World War II led to the pragmatic approach by Sverdrup and Munk (1947), whose aim was to provide a first-hand estimate of the wave conditions to be expected under given fetch, duration, and wind speed conditions. With new impetus after the war, and under the criticism of Ursell (1956), the first consistent explanation of wind wave generation and growth was provided by the two practically parallel papers by Phillips (1957) and Miles (1957). Much further attention has then been given to further developments, as described in the classical references by Janssen (1991), Komen et al. (1994), and Ardhuin et al. (2010). In more recent times, Pizzo et al. (2021) provide a beautiful picture of the past and present situation. However, our focus is strictly on the very first stages of generation, avoiding the complexity of the open ocean and its big waves. Therefore, for our discussion we will focus on Phillips (1957) and Miles (1957), as they suffice for our purposes.

The two explanations were complementary to each other, with the Phillips theory providing (by surface pressure fluctuations) the initial small wave amplitudes on which the Miles feedback mechanism could then act. Nowadays the problem is ignored in most regular applications because either a background low white spectrum, or a minimal spectrum dependent on the local wind speed are assumed. Of course this initial range is what we are interested in. Starting from a calm flat surface, the initial sequence can be seen in a wind wave tank (Benetazzo et al. 2019). When wind begins to blow (represented in practice by a 1-s step function), for several seconds nothing seems to happen and only an increasing drift of the surface is evident. Then, very low and short corrugations appear for a little while before developing into more familiar, still very small, waves.

In this respect see the detailed laboratory description by Zavadsky and Shemer (2017). The example in Fig. 5, with a wind speed 6 m s^{-1}, is from the wind wave tank of the First Institute of Oceanography (Qingdao, China). Actually two theories compete for the appearance of the first wavelets. After the classical Phillips (1957) theory, Kawai (1979) proposed a different approach based on a sort of Kelvin–Helmholtz
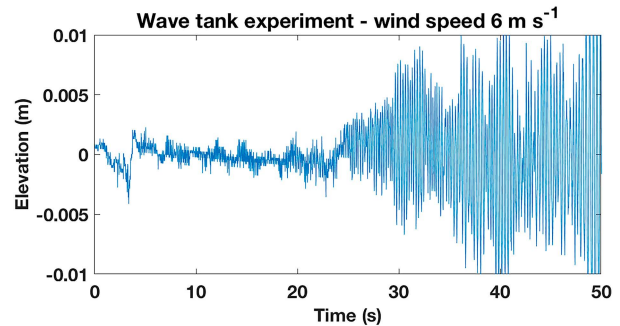

Fig. 5. Initial stages of wind wave generation and evolution in a wind wave tank. Wind speed is 6 m s^{-1}.

(KH) instability associated with the strong vertical shear present immediately below the water surface (see also Miles 1959; Zavadsky and Shemer 2017). The ensuing turbulence leads to the initial surface corrugations with wavelength 2–3 cm. As stressed by Kawai (1979), the frequency, hence wavelength, of the initial wavelets coincides with the frequency of the waves with maximum growth rate as expected from the shear flow instability. More on this aspect of the problem can be found in the general discussion of section 6.

As regards the historically debated question of the minimal wind speed for wave generation (Mitsuyasu 2002), our tests on the tower provided evidence in this direction, also with indications (see section 5) that the reply is not unique.

4. The measurements

The data we report were recorded on three days, 20, 23, and 25 June 2008. See the discussion in section 6 for the reasons for this delayed analysis. On these days, the weather was characterized by clear and sunny conditions, with no synoptic wind, hence no relevant wind waves or distant swells, given the closed nature of the Adriatic Sea. Often there were limited patches of low waves, 10 cm high and 3–4-s periods, hence 15–25 m long, which only marginally affected the possible trigger of the initial wavelets (see the later discussion).

A summary of the conditions on the three days of June 2008 is as follows:

- 20 June: Early breeze from northeast, then calm, with a following minimal breeze from southeast (the expected direction). The wind was coming and going, with 2 m s^{-1} speed or less. The general situation was some background, a few centimeter-high waves, with ripples of early generation.
- 23 June: Similar background waves, 3-s period. Some breeze from northeast in the early morning, then the expected southeast breeze, progressively growing from 2 to 3.5 m s^{-1}. Breeze stable until 1600 local time (LT) with waves approaching a steady state.
- 25 June: The area of sea breeze is progressively extending from land toward the tower in an otherwise rather calm sea, with some very low background of relatively long waves. After the local passage of the front, wind speed was first at 1.8 m s^{-1} (early stages of wave generation), then steady at 3.2 m s^{-1}. Records halted at about 1600 LT.
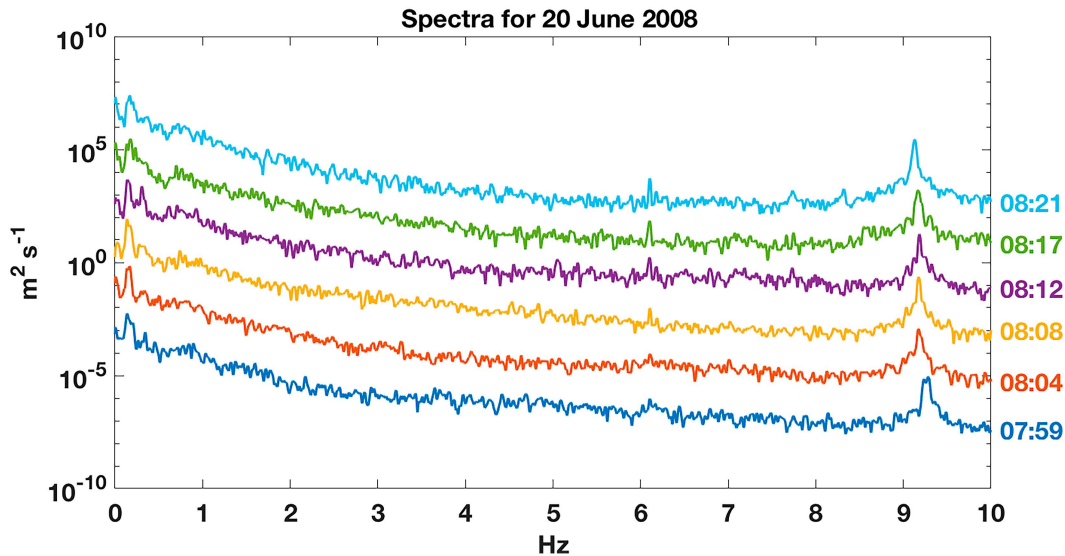
FIG. 6. Log-linear wave spectra in the early morning of 20 Jun 2008. Note the background wave field and the sharp peak of the earliest stages of generation by local breeze. The time of each record is on the right. The energy scale is correct for the first 0759 LT spectrum. The energy of each sequential spectrum is multiplied by 100 for better visualization.

Most of the records lasted 5 min. At the regime conditions of day 25, we extended their duration to 10 min. Except for two short periods with speed close to 0.20 m s^{-1}, most of the time surface current was absent or negligible.

5. Results

We outline here our main results, again following the days of June 2008.

For 20 June, the results of this set of data are not good for the estimate of the actual growth, but they are well representative of the minimal wind speed for "wave" generation (we use quotation marks for the different meaning one can give to actual waves). In Fig. 6 we show six consecutive spectra taken in less than half an hour (the nominal 5 min actually lasted 4 min 36 s). The wind speed was 1.8 m s^{-1}. The scale in the figure is log-linear to show the range of frequency (from 0 to 10 Hz) better, the background low-frequency noise and the sharp peak at a practically steady 9.2 Hz, which is the main feature of interest. This peak is present also in all the following spectra taken during the overall 90 min, which neither grows nor disappears. We interpret this as the minimal wind speed for wavelet generation, but not strong enough to make them grow further. We will discuss this more in the next section.

For 23 June, the initial stage of wave generation and growth is well represented in Fig. 7. Within the present background noise, there is an evident growth of the wavelets contribution. This represents well the typical waves evolution for these mild wind speeds. We are only slightly above the threshold seen on day 20 (here we are at 2.2 m s^{-1}), and this is sufficient to make wavelets grow, shifting their peak to progressively lower frequency. The details are better seen in Fig. 8 focused with a linear scale on the 6–9-Hz range of the spectrum.

Granted some small variations that we associate to minor ones of the wind speed and to the confidence limits of the measured data, there is a progressive shift toward both a lower frequency and higher related wave heights. Note the different vertical scales in the various panels and the corresponding wave height (mm, referred to the considered frequency range) on the right of each panel. For the 2.2 m s^{-1} wind in this period, the shift of the dominant frequency was from 8.0 to 6.5 Hz, while the significant wave height increased from 4 to 15 mm in 25 min. However, when (relatively speaking) wind speed grows to 3–3.5 m s^{-1}, as in the afternoon, and the related waves grow as well, the wavelets disappear. The reason for this is discussed in the next section.

At this higher speed, the evolution is more similar to the classical one we are used to. This is shown in Fig. 9a, where the reported significant wave height H_s refers only to the local growing wind sea (we consider here only energy above 0.3 Hz). This set of records refers to the afternoon when a sustained sea breeze set up, blowing for at least a couple of hours. We see the steadily growing H_s and the progressive decrease of the related peak frequency.

For 25 June, the general situation and evolution are very similar to day 23. There is a very light breeze at the beginning, 1.8 m s^{-1}, with the expected wavelets at 9 Hz. These progressively disappear with the growth of the sea breeze wind waves. As for day 23, Fig. 9b shows the progressive evolution of the related significant wave height and peak frequency.

6. Discussion

The breeze conditions for our measurements were not the intense ones that had originally triggered our interest. However, just these very light breezes led us to focus on different,
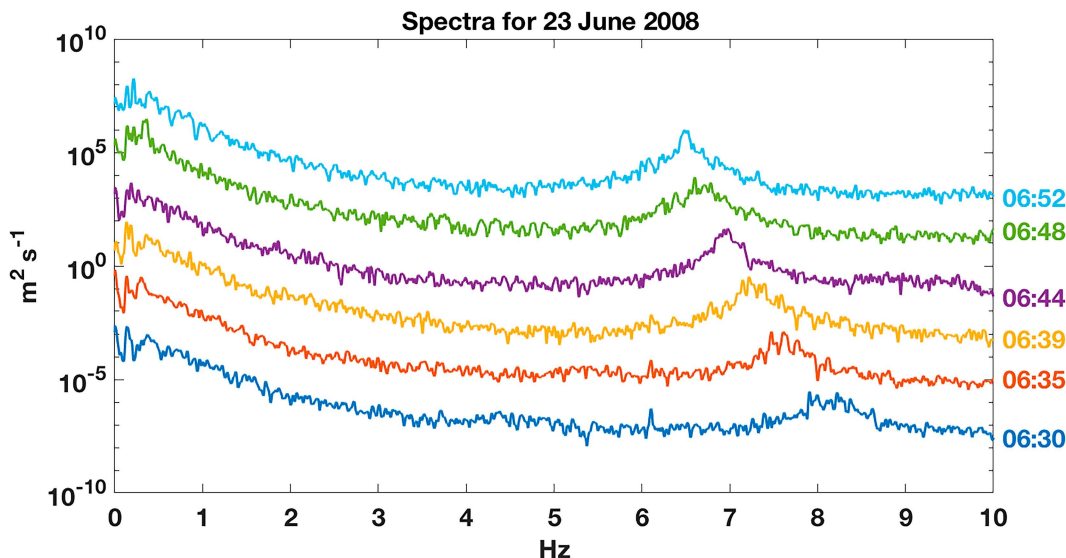
FIG. 7. As in Fig. 6, but for 23 Jun 2008. Note in this case the progressive shift of the breeze waves toward lower frequencies. See Fig. 8 for better details.

but still interesting, aspects of the problem. We discuss in order 1) the minimum wind speed for waves generation, 2) the two possible processes for the appearance of the first wavelets, 3) the growth rate of the associated high-frequency components, 4) their "fully developed conditions," and 5) the presence, or absence, of high-frequency ripples on more developed, still sea breeze, waves. We conclude discussing the progressive weakening, in the years, of the intensity of sea breezes and the associated climate reasons.

a. The minimum wind speed for waves generation

Discussing wind waves generation in section 3, we had cited Kawai (1979) for the explanation of the first 2–3-cm-long wavelets appearing on the surface soon after the wind begins to blow. A historically debated question is the minimal wind speed for waves generation (see, e.g., Mitsuyasu 2002). Within the confidence limits of the local environmental conditions, our results at the tower suggest 1.8 m s^{-1} as the minimal one at which wavelets appear on the surface. This is consistent with the very detailed experimental data by Donelan and Plant (2009). The ensuing 9-Hz, 2.5-cm-long wavelets indicate the limit below which (Hz) the direct interaction with, and input from, the atmosphere (Miles 1959) is larger than the viscosity dissipation, allowing the wavelets to grow, slowly at the beginning and more and more rapidly with time, in both length and height. In their keen experiment Donelan and Plant (2009) and Zavadsky and Shemer (2017) have explored various and different conditions, e.g., changing temperatures or distinguishing between slowly growing or impulsive wind speeds. Our 1.8 m s^{-1} minimal wind speed for wave generation appears typical for the described (very stable) conditions. In the unstable conditions that characterize, e.g., the fall, when the first northerly winds blow over a still warm sea, our experience suggests that this threshold wind speed can be

even (slightly) lower. However, we do not have a rigorous documentation for this.

b. The two possible processes for the appearance of the first wavelets

In section 3 we mentioned the two processes, Phillips (1957) and Kawai (1979), considered for the generation of the first wavelets on an otherwise flat or smooth sea surface. What Phillips considered is the resonance between the pressure oscillations on the blowing surface wind and the wavelength and phase speed of the resonant wavelets. Kawai focused on the horizontal drag by wind on the water surface. This creates a very thin surface current. The ensuing vertical gradient leads to instability, hence turbulence, hence surface corrugations. In this respect, Phillips went further by assuming that, with the increasing wavelengths hence periods, the correspondingly stronger and larger air pressure oscillations could contribute to the substantial development of stormy waves. As it was quickly established when the first wave models were developed and compared (see The SWAMP Group 1985), the Phillips processes contribution turns out to be negligible with respect to the one suggested by Miles (1957). Indeed, a quick estimate following the amply used Cavaleri and Malanotte-Rizzoli (1981) formulation ($c_D = 0.0012$, $\sigma = 2\pi \times 5.0$, $k = 2\pi/0.05$) suggests the Phillips process to be low by orders of magnitude.

Focusing our attention on the first wavelets, the Phillips and Kawai approaches are not necessarily an "either or" situation, since they are both physically sound. Rather, it is a matter of quantification depending on the local conditions. Indeed, in very light winds, as the ones described in the previous section, on pure intuitive ground we feel that it is the Phillips process that is likely to give the first wavelets. In this respect, it is instructive to see the physical evidence (the sea surface) in Fig. 10 (left) and the 2D spectrum in right panel.
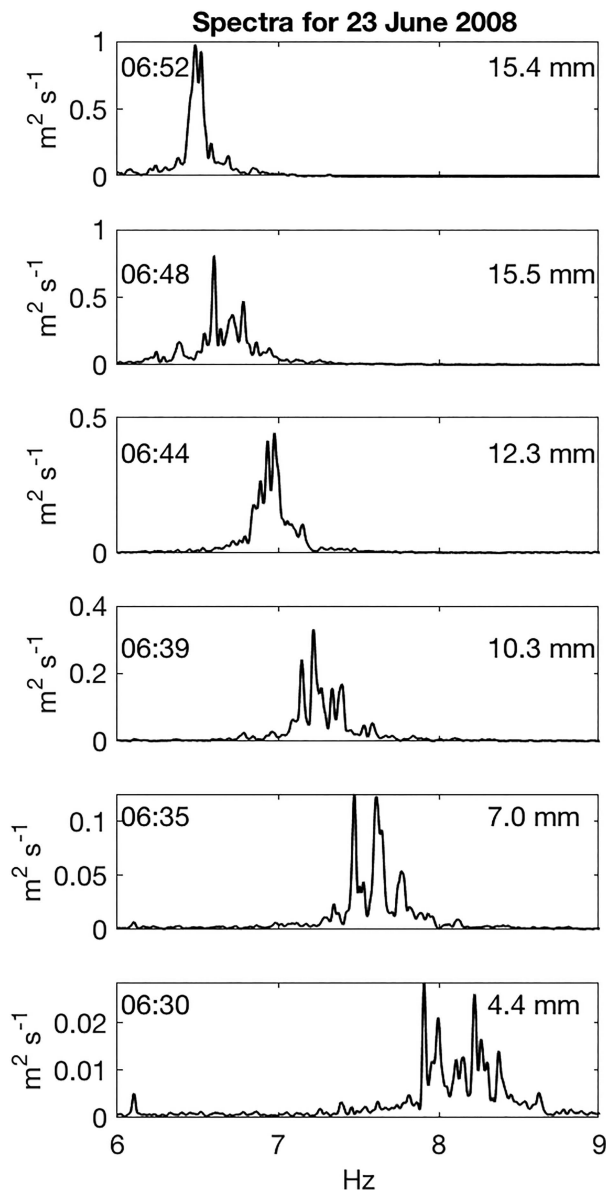
FIG. 8. Linear-linear spectra of the breeze waves spectra seen in Fig. 7. The vertical scale is in 10^{-4} units. The inner numbers show the time of the record (at left) and the significant wave height (mm) corresponding to the shown part of the spectrum (at right).

The corresponding 1D spectrum (see Fig. 7) is the 0648 LT one of 23 June. In the left panel of Fig. 10, the wind is from the right to the left, and it is easy to recognize the two wave systems at almost cross angles, symmetrical with respect to the wind flow direction. This is macroscopically represented in the 2D spectrum, with the two lobes of energy at slightly more than 90°. Note that the 0° spectra flow direction corresponds to the flow ones of the sea breeze, i.e., from right to left in the scheme of Fig. 4. This strongly supports the Phillips approach.

With a stronger wind, we suggest that the Kawai process becomes the leading one, although always for the very early stages before the Miles theory steps in. However, we believe

time should also be considered. With a sudden 6 m s^{-1} wind, as in the wind wave tank example of Fig. 3, there is no time for the wind-drifted surface layer to drag rapidly along the lower layers, and instability arises. However, if, starting from a no wind condition, the wind speed grows slowly, the upper layer will have the time to drag along the lower ones with a substantial decrease of the vertical gradient, hence the possible instability. Therefore, the issue of whether Phillips or Kawai prevails is a delicate balance of wind speed and its time gradient. We should never forget we are talking of the open sea, where ideal conditions are rare, and small details can flip the prevailing situation. Note also that it is very difficult to see the Phillips wavelets in a wind wave channel. Granted that most of the tests are there done with substantial wind speeds, also for low ones, the wind and therefore the surface pressure fields are strongly affected by the input grid, thereby disrupting the delicate conditions for the Phillips process.

c. The growth rate of the high-frequency components

Granted the presence of the initial wavelets on the surface, as soon as wind speed is (in our case) above the 1.8 m s^{-1} threshold limit, more energy is fed into the waves that begin to grow in height and length. This provides a progressively enhanced input by wind and a relatively reduced viscous dissipation, hence an enhanced growth. This progressively shifts the waves system into the more familiar range of a growing sea where the dynamical equilibrium is now between generation and the classical dissipation, the latter due mainly to (white-)capping. Indeed, Sutherland and Melville (2015) have shown that wave energy dissipation is due also to microbreakers, not easily detected by standard optimal means. As wavelets grow in height and length, these breakers do appear as soon as surface tension allows, with a progressive shift of the dynamical equilibrium of the forces at play.

d. "Fully developed conditions"

We put this title between quotation marks to keep track of the very low wave heights we are dealing with. In any case, as soon as we move away from the "viscous" regime, waves, albeit small, do evolve following the familiar pattern we have seen in Figs. 8 and 9. The fully developed conditions described by Pierson and Moskowitz (1964) (PM) were derived for severe open ocean conditions, in practice for wind speed greater than 10 m s^{-1}. It is interesting that, although with some approximation, their suggested formula for H_s in fully developed conditions, $H_s = 2.2 \times (U_{10}/10)^2$ with U_{10} being the classical wind speed, works also for our data, more specifically for 23 and 25 June. In these two days the maximum measured H_s were close to 0.2 m, to be compared to the 0.20–0.25 m derived with the PM formula, using our measured wind speed. Granted its approximation for these limited wind and wave regimes, the fit suggests that, mutatis mutandis, at these generation conditions we are already at, or close to, the classical situation we envisage for wind wave generation. Indeed, also the 2D spectra we derived for the well-developed conditions are similar to the classical ones we are used to seeing for a wind sea.
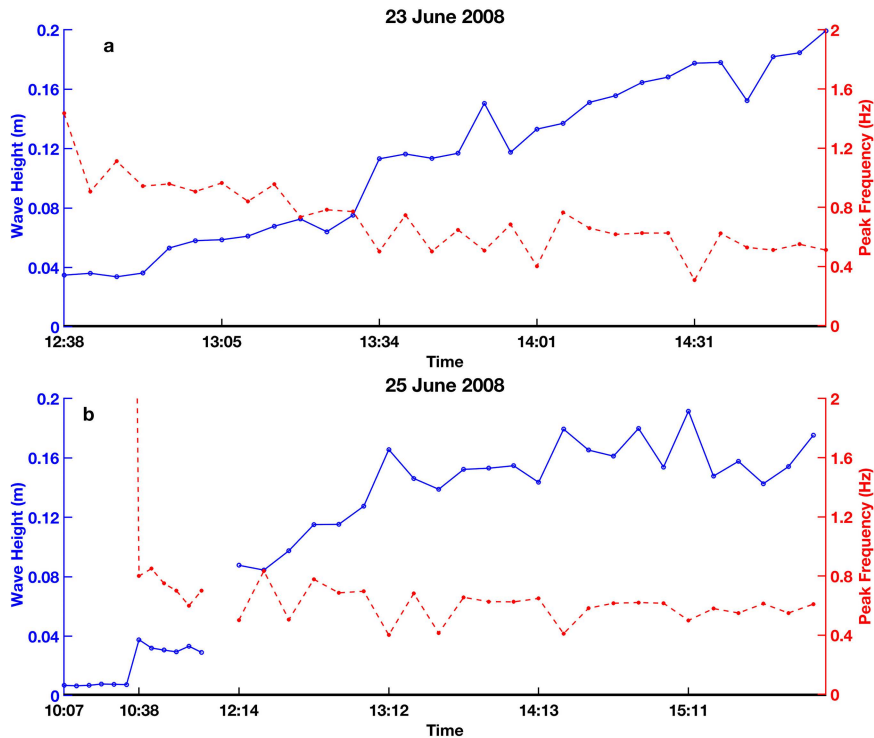
FIG. 9. Time evolution of the significant wave height and peak period of the sea breeze generated waves for (a) 23 and (b) 25 Jun 2008. Note the discontinuity in the time for 25 June.

e. The presence, or absence, of high-frequency ripples on more developed waves

During measurements, as macroscopically in our records, wavelets are present only in the earliest stages of generation that we considered. We stress that we keep talking only of active waves of height 0.20 m or less. In practice, starting from a flat surface with wind blowing at, e.g., 3 m s^{-1}, we see wavelets in their earliest phases of generation, after which they disappear, both from direct evidence and the records. Figure 11 exemplifies the situation with two records taken at 4-h difference. The figure reports both the two spectra and the
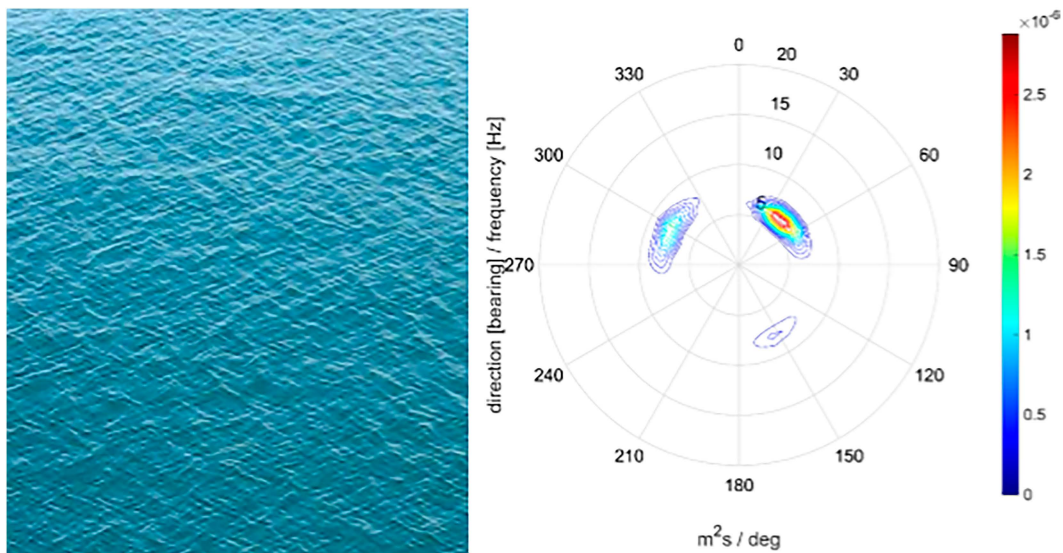

FIG. 10. (left) View of an early generative sea with initial crossed ripples. (right) The 2D spectrum of the corresponding wave conditions at 0648 LT 23 Jun. See Fig. 7 for the 1D spectrum.
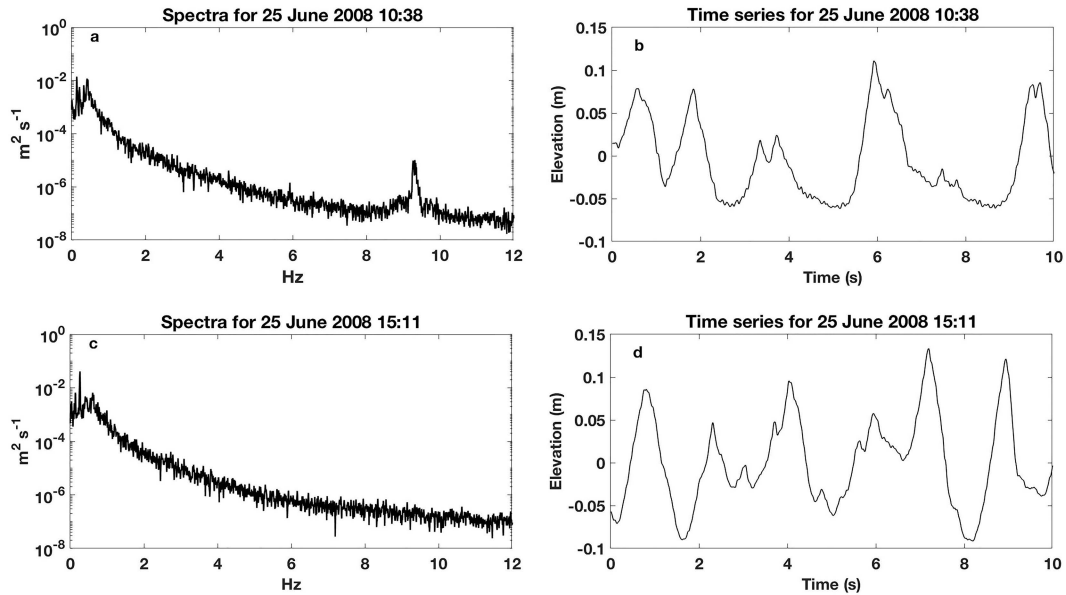
FIG. 11. Log-linear spectra and a sample of the recorded time series for (a),(b) one of the early 25 Jun 2008 records and (c),(d) later in the day. Note the wavelet peak in the spectrum in (a) [missing in (c)] and the corresponding little "noise" throughout the signal in (b). This "noise" is absent in (d) when the sea breeze waves have begun to develop.

corresponding surface records. The wavelets are present in the earlier record with only longer background waves (Figs. 11a,b), but absent in the latter one (Figs. 11c,d) when, with respect to the background, the now grown breeze waves have a shorter period, hence length. We argue that the spatial and temporal gradients of a developing sea, once this has stepped in, impedes the formation of the wavelets, at least the ones following the suggested KH instability. The wind generated water skin currents and the consequent vertical shear are steadily destroyed by the rapidly alternating stretching and compressing orbital velocity. On the contrary, a low and longer wave background has in this respect no or limited effect. Following linear theory, a 0.10-m-high 5-s wave has an orbital velocity horizontal spatial gradient of 0.006 m s^{-1} m^{-1}. For a 0.15-m-high 1.6-s wave this value jumps to 0.3 m s^{-1} m^{-1}, almost two orders of magnitude larger. We hypothesize that in these latter conditions strong spatial and temporal gradients of the wave surface orbital velocity impede the formation of the consequences of KH instability. This raises the question of where the ripples used by scatterometers come from. Our suggested explanation is that in an active and growing sea the orbital velocity gradients are inversely proportional to the wave period, or, in other words, to the square root of the wave height. Therefore, the gradients tend to decrease in the more advanced stages of generation, which, however, were not reached at the Acqua Alta tower.

We conclude with a short comment and some information on the local sea breezes. Breezes were very strong 60–70 years ago, blowing sand violently across the beach. Later on, during the early years of the Acqua Alta tower, set into position in March 1970, in early summer the "sirocco gordo," a local dialect expression for "greedy southeast wind" (the strong breeze), was the norm, with prolonged sustained wind speeds (see Fig. 1) on the order of 6–7 m s^{-1}. The sea was choppy.

All this has now disappeared. So, conceived with our previous experience, the experiment had to be carried out with much reduced wind speeds. Indeed, after conceiving and preparing the experiment, we had to wait a couple of years to find suitable conditions, although these were still pale reproductions of what was present years (decades) ago. Note that we tried and were ready on board a few times before finding the relatively good days and moments. The reason for this is the less and less cold temperature of the northern Adriatic Sea (that we monitor at the tower), in the specific case representative of the milder and milder winters. See in this respect Raicich and Colucci (2019) for a trend since 1900. The warmer the sea, the less the land–sea temperature difference, hence the milder the sea breezes. We consider this as a representative parameter and a consequence of local climate change.

A final comment on why we waited 10+ years for a detailed analysis of the available data. Apart from other commitments, we were always hoping for a stroke of luck and more and better conditions, hence measurements. The restoration of the tower finally made this not possible, hence the, albeit late, convergence.

7. Summary

We itemize in the following our main findings.

1) Provided the background wave conditions are low enough, sea breezes offer the possibility of time-limited generation in the open sea.

2) The minimum wind speed for wind wave generation is close to 1.8 m s^{-1}. This result holds for stable air–sea stability conditions. We have indications from previous experience for a slightly smaller wind speed in unstable air–sea

conditions. The threshold may also depend on the already existing short period waves that, if not very low and long, may push up the minimal wind speed for generation (see item 8).

3) In all our cases the wind speed was uniform from about 8-m height to the sea surface. Evidence from the literature suggests that in these conditions the Miles critical layer was practically adjacent to the waves surface.

4) We suggest that the first wavelets appear following the Phillips resonance mechanism and/or the Kelvin–Helmholtz instability in the vertically sheared wind driven current layer. Which process prevails depends on the wind speed, with Phillips being more likely in very low wind speed conditions, especially under a very slowly growing wind speed.

5) In our stable conditions, if the wind speed remains around 1.8 m s^{-1}, wavelets appear, but they do not evolve into longer and higher wind waves.

6) For higher wind speeds, wavelets evolve into classical wind waves.

7) For the local wind speeds of 3.0–3.5 m s^{-1}, the breeze extent and duration allow the development of practically fully developed conditions. The results fit with good approximation the practical rule derived from the more classical and certainly more severe cases.

8) Wavelets are present in the earliest stages of generation. As soon as developed as young wind waves, the active wind sea impedes their formation. We suggest this is due to the strong spatial and temporal gradients associated with the surface orbital velocity that impedes the formation of the Kelvin–Helmholtz instability in the vertically sheared wind driven surface current layer. With waves further growing, their increased height, period, and hence length, lead to correspondingly reduced gradients allowing wavelets to appear again at more developed conditions.

9) The long-term decrease of the sea breeze intensity in our area of interest is associated with a steadily warmer and warmer sea at the end of the winter season, a suggestive indication of climate change.

REFERENCES

Aboobacker, V. M., M. Seemanth, S. V. Samiksha, K. Sudeesh, J. Kerbar, and P. Vethamony, 2014: Sea breeze-induced wind wave growth in the central west coast of India. *Ocean Eng.*, **84**, 20–28, https://doi.org/10.1016/j.oceaneng.2014.03.030.

Ardhuin, F., and Coauthors, 2010: Semiempirical dissipation source function for ocean waves. Part 1: Definitions, calibration and validations. *J. Phys. Oceanogr.*, **40**, 1917–1941, https://doi.org/10.1175/2010JPO4324.1.

Babanin, A. V., M. L. Banner, I. R. Young, and M. A. Donelan, 2007: Wave follower measurements of the wind input spectral function. Part 3. Parameterization of wind input enhancement due to wave breaking. *J. Phys. Oceanogr.*, **37**, 2764–2775, https://doi.org/10.1175/2007JPO3757.1.

Benetazzo, A., L. Cavaleri, H. Ma, S. Jiang, F. Bergamasco, W. Jiang, S. Chen, and F. Qiao, 2019: Analysis of the effect of fish oil on wind waves and implications for air-water interaction studies. *Ocean Sci.*, **15**, 725–743, https://doi.org/10.5194/os-15-725-2019.

Carpenter, J. R., M. P. Buckley, and F. Veron, 2022: Evidence of the critical layer mechanism in growing wind waves. *J. Fluid Mech.*, **948**, A26, https://doi.org/10.1017/jfm.2022.714.

Cavaleri, L., and P. Malanotte Rizzoli, 1981: Wind wave prediction in shallow water – Theory and applications. *J. Geophys. Res.*, **86**, 10 961–10 973, https://doi.org/10.1029/JC086iC11p10961.

——, and S. Zecchetto, 1987: Reynolds stresses under wind waves. *J. Geophys. Res.*, **92**, 3894–3904, https://doi.org/10.1029/JC092iC04p03894.

——, P. Piantà, and G. Iuso, 1985: Influence of a sea structure on the surrounding wind field. *Nuovo Cimento*, **7**, 440–446, https://doi.org/10.1007/BF02507284.

——, L. Bertotti, R. Buizza, A. Buzzi, V. Masato, G. Umgiesser, and M. Zampato, 2010: Predictability of extreme meteo-oceanographic events in the Adriatic Sea. *Quart. J. Roy. Meteor. Soc.*, **136**, 400–413, https://doi.org/10.1002/qj.567.

——, and Coauthors, 2019: The October 29, 2018 storm in Northern Italy – An exceptional event and its modelling. *Prog. Oceanogr.*, **178**, 102178, https://doi.org/10.1016/j.pocean.2019.102178.

——, and Coauthors, 2020: The 2019 flooding of Venice and its implications for future predictions. *Oceanography*, **33** (1), 42–49, https://doi.org/10.5670/oceanog.2020.105.

Donelan, M. A., and W. J. Plant, 2009: A threshold for wind-wave growth. *J. Geophys. Res.*, **114**, C07012, https://doi.org/10.1029/2008JC005238.

Hasselmann, L., and Coauthors, 1973: Measurements of wind-wave growth and swell decay during the Joint North Sea Wave Project (JONSWAP). *Dtsch. Hydrogr. Z. Suppl.*, **A8** (12), 1–93.

Janssen, P. A. E. M., 1991: Quasi-linear theory of wind-wave generation applied to wave forecasting. *J. Phys. Oceanogr.*, **21**, 1631–1642, https://doi.org/10.1175/1520-0485(1991)021<1631:QLTOWW>2.0.CO;2.

Jeffreys, H., 1925: On the formation of water waves by wind. *Proc. Roy. Soc. London*, **107**, 189–206, https://doi.org/10.1098/rspa.1925.0015.

Kawai, S., 1979: Generation of initial wavelets by instability of a coupled shear flow and their evolution to wind waves. *J. Fluid Mech.*, **93**, 661–703, https://doi.org/10.1017/S0022112079000197X.

Komen, G. J., L. Cavaleri, M. Donelan, K. Hasselmann, S. Hasselmann, and P. A. E. M. Janssen, 1994: *Dynamics and Modelling of Ocean Waves*. Cambridge University Press, 532 pp.

Miles, J. W., 1957: On the generation of surface waves by shear flows. *J. Fluid Mech.*, **3**, 185–204, https://doi.org/10.1017/S0022112057000567.

——, 1959: On the generation of surface waves by shear flows Part 3. Kelvin-Helmholtz instability. *J. Fluid Mech.*, **6**, 583–598, https://doi.org/10.1017/S0022112059000842.

Miller, S. T. K., B. D. Keim, R. W. Talbot, and H. Mao, 2003: Sea breezes: Structure, forecasting and impacts. *Rev. Geophys.*, **41**, 1001, https://doi.org/10.1029/2003RG000124.

Mitsuyasu, H., 2002: A historical note on the study of ocean surface waves. *J. Oceanogr.*, **58**, 109–120, https://doi.org/10.1023/A:1015880802272.

Phillips, O. M., 1957: On the generation of waves by turbulent wind. *J. Fluid Mech.*, **2**, 417–445, https://doi.org/10.1017/S0022112057000233.

Pierson, W. J., and L. Moskowitz, 1964: A proposed spectral form for fully developed wind seas based on the similarity theory of S. A. Kitaigorodskii. *J. Geophys. Res.*, **69**, 5181–5190, https://doi.org/10.1029/JZ069i024p05181.

Pizzo, N., L. Deike, and A. Ayet, 2021: How does wind generate waves? *Phys. Today*, **74**, 38–43, https://doi.org/10.1063/PT.3.4880.

Rafiq, S., C. Pattiaratchi, and I. Janekovic, 2020: Dynamics of the land-sea breeze system and the surface current response in South-West Australia. *J. Mar. Sc. Eng.*, **8**, 931, https://doi.org/10.3390/jmse8110931.

Raicich, F., and R. R. Colucci, 2019: A near-surface sea temperature time series from Trieste, northern Adriatic Sea (1899–2015). *Earth Syst. Sci. Data*, **11**, 761–768, https://doi.org/10.5194/essd-11-761-2019.

Sauer, K. D., and J. P. Allebach, 1987: Iterative reconstruction of multidimensional signals from nonuniformly spaced sample. *IEEE Trans. Circuits Syst.*, **34**, 1497–1506, https://doi.org/10.1109/TCS.1987.1086088.

Snyder, R. L., F. W. Dobson, J. A. Elliott, and R. B. Long, 1981: Array measurements of atmospheric pressure fluctuations above surface gravity waves. *J. Fluid Mech.*, **102**, 1–59, https://doi.org/10.1017/S0022112081002528.

Sutherland, P., and W. K. Melville, 2015: Field measurements of surface and near-surface turbulence in the presence of breaking waves. *J. Phys. Oceanogr.*, **45**, 943–965, https://doi.org/10.1175/JPO-D-14-0133.1.

Sverdrup, H. U., and W. H. Munk, 1947: *Wind, Sea and Swell: Theory of Relations for Forecasting.* Hydrographic Office, 44 pp.

The SWAMP Group, 1985: *Ocean Wave Modeling.* Plenum Press, 256 pp., https://doi.org/10.1126/science.229.4711.377.a.

Ursell, F., 1956: Wave generation by wind. *Surveys in Mechanics*, G. K. Batchelor and R. M. Davies, Eds., Cambridge University Press, 216–249.

Zavadsky, A., and L. Shemer, 2017: Water waves excited by near-impulsive wind forcing. *J. Fluid Mech.*, **828**, 459–495, https://doi.org/10.1017/jfm.2017.521.